Electronic Supplementary Information (ESI)

Key properties of Ni-MgO-CeO_2, Ni-MgO-ZrO_2, and Ni-MgO-$Ce_{(1-x)}Zr_{(x)}O_2$, catalysts for the reforming of methane with carbon dioxide

Won-Jun Jang[a], Hak-Min Kim[a], Jae-Oh Shim[a], Seong-Yeun Yoo[a], Kyung-Won Jeon[a], Hyun-Suk Na[a], Yeol-Lim Lee[a], Dae-Woon Jeong[b], Jong Wook Bae[c], In Wook Nah[d], Hyun-Seog Roh[a,*]

[a] *Department of Environmental Engineering, Yonsei University, 1 Yonseidae-gil, Wonju, Gangwon 220-710, Republic of Korea*

[b] *School of Civil, Environmental and Chemical Engineering, Changwon National University, 20 Changwondaehak-ro, Changwon, Gyeongnam 51140, Republic of Korea*

[c] *School of Chemical Engineering, Sungkyunkwan University (SKKU), 2066 Seobu-ro, Suwon, Gyeonggi-do 16419, Republic of Korea*

[d] *Center for Energy Convergence, Korea Institute of Science and Technology (KIST), 5 Hwarang-ro 14-Gil, Seongbuk-gu, Seoul 02792, Republic of Korea*

Table S1

Characteristics of Ni-MgO-CeO_2, Ni-MgO-ZrO_2, and Ni-MgO-$Ce_{(1-x)}Zr_{(x)}O_2$ catalysts

Description	Linear combination fitting[a]		Area of XPS spectra[b]	
	NiO	Ni^0	*u‴*	Ce3d
Ni-MgO-CeO_2	0.60	0.40	4552	49362
Ni-MgO-$Ce_{0.8}Zr_{0.2}O_2$	0.49	0.51	3395	41154
Ni-MgO-$Ce_{0.6}Zr_{0.4}O_2$	0.44	0.56	1458	25636
Ni-MgO-$Ce_{0.4}Zr_{0.6}O_2$	0.29	0.71	1607	20628
Ni-MgO-$Ce_{0.2}Zr_{0.8}O_2$	0.17	0.83	1774	17040
Ni-MgO-ZrO_2	0.08	0.92	-	-

[a] Referring to Fig. 4.
[b] Referring to Fig. S6.

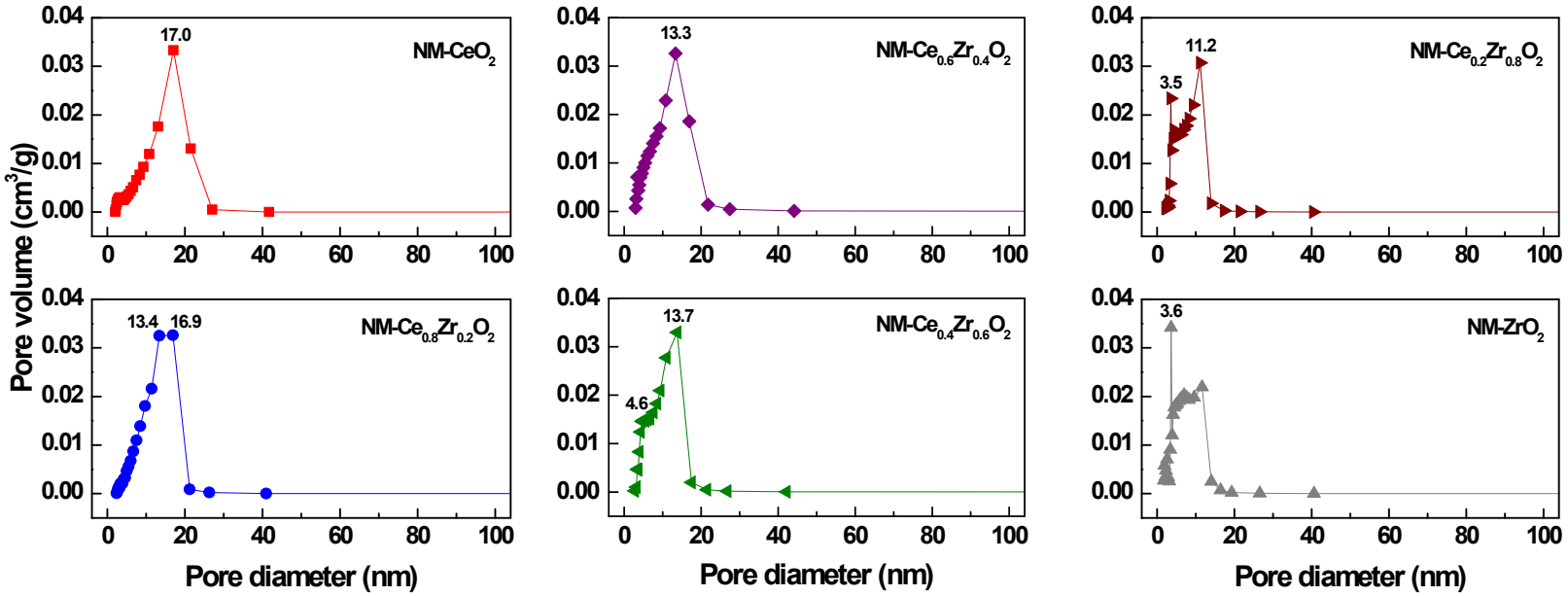

Fig. S1. Pore distribution of NM-CeO_2, NM-ZrO_2, and NM-$Ce_{(1-x)}Zr_{(x)}O_2$ catalysts.

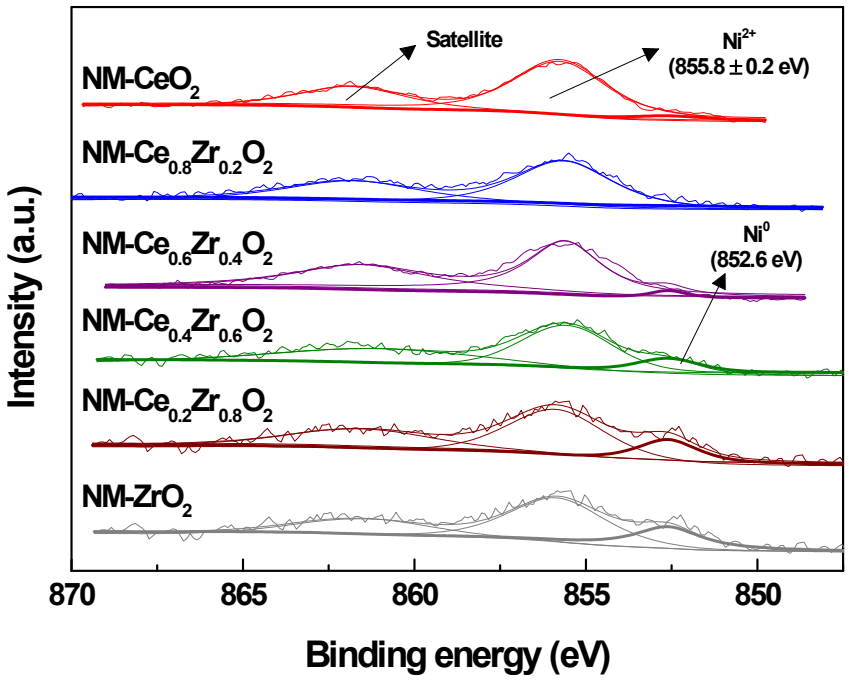

Fig. S2. XPS spectra of Ni2p3/2 in Ni-MgO-CeO_2, Ni-MgO-ZrO_2, and Ni-MgO-$Ce_{(1-x)}Zr_{(x)}O_2$ catalysts.

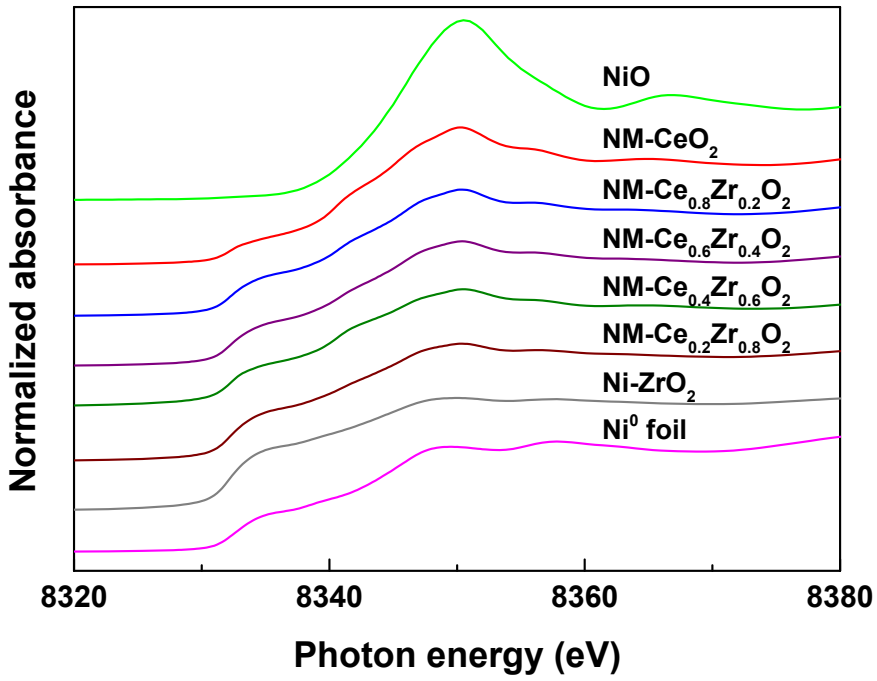

Fig. S3. XANES spectra over Ni-MgO-CeO_2, Ni-MgO-ZrO_2, Ni-MgO-$Ce_{(1-x)}Zr_{(x)}O_2$ catalysts, and references (NiO and Ni foil).

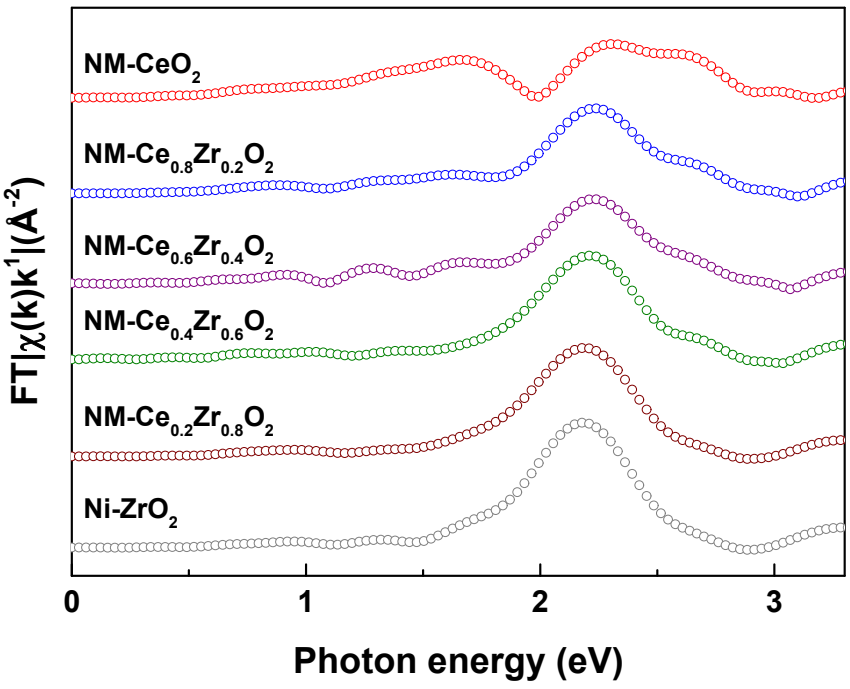

Fig. S4. k^1 weighted Fourier-transformed EXAFS spectra over Ni-MgO-CeO_2, Ni-MgO-ZrO_2, Ni-MgO-$Ce_{(1-x)}Zr_{(x)}O_2$ catalysts, and references (NiO and Ni foil).

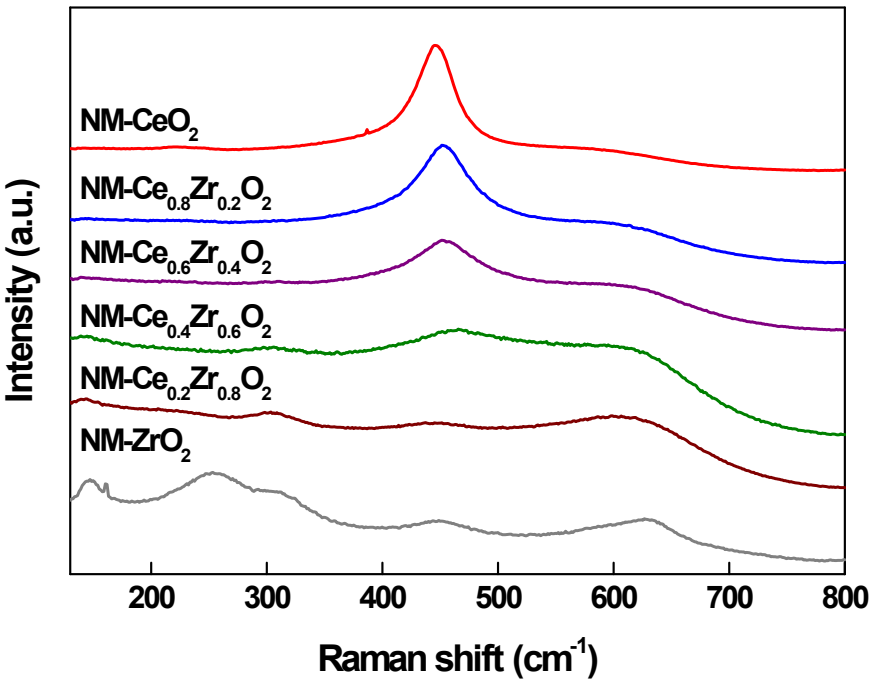

Fig. S5. Raman spectra of Ni-MgO-CeO_2, Ni-MgO-ZrO_2, and Ni-MgO-$Ce_{(1-x)}Zr_{(x)}O_2$ catalysts.

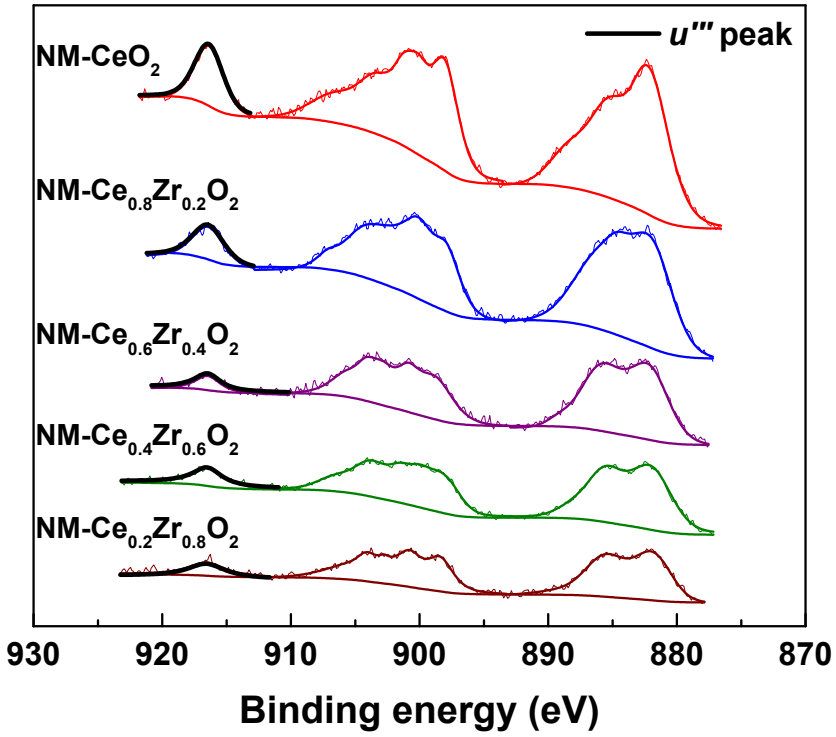

Fig. S6. Curve fits for the *u'''* peak of Ce3d XPS spectra over Ni-MgO-CeO_2, Ni-MgO-ZrO_2, and Ni-MgO-$Ce_{(1-x)}Zr_{(x)}O_2$ catalysts.

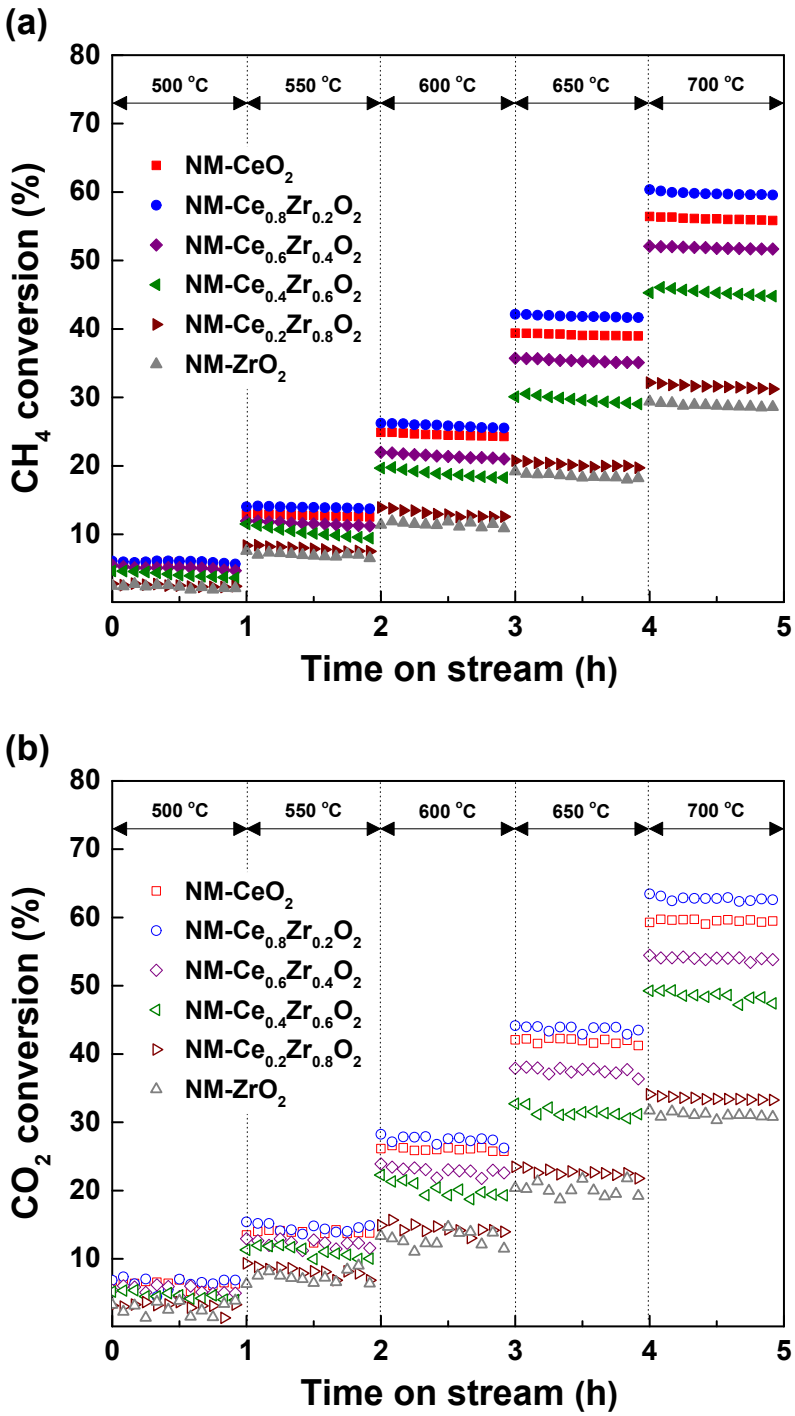

Fig. S7. CH_4 and CO_2 conversions over NM-CeO_2, NM-ZrO_2, and NM-$Ce_{(1-x)}Zr_{(x)}O_2$ catalysts as a function of reaction temperatures from 500 to 700 °C (CH_4:CO_2:N_2 = 1:1:1 and GHSV = 675,000 mL·g^{-1}·h^{-1}).

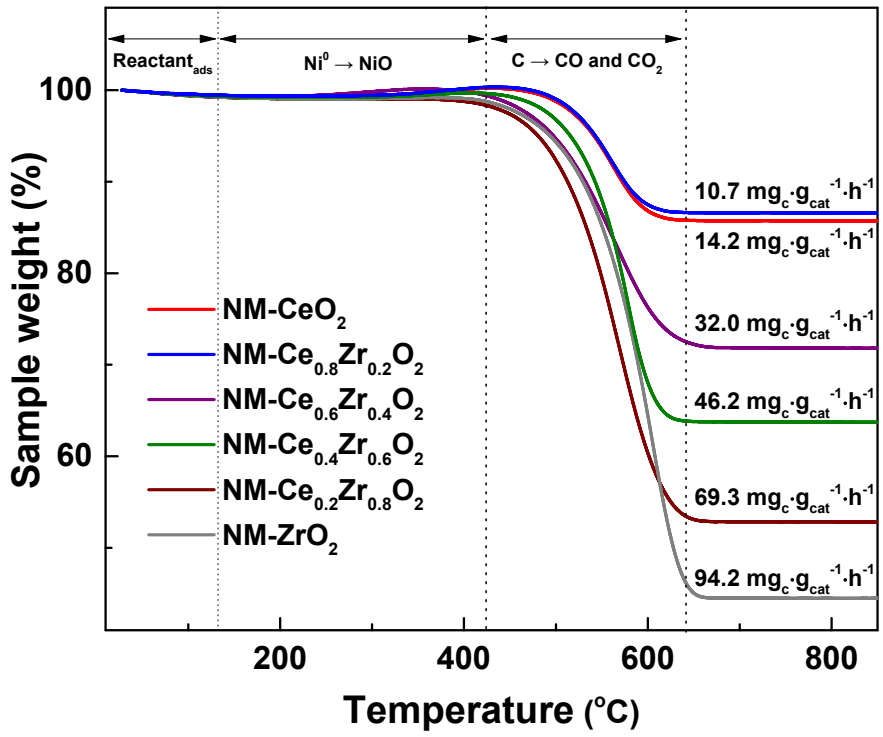

Fig. S8. TGA profiles of NM-CeO_2, NM-ZrO_2, and NM-$Ce_{(1-x)}Zr_{(x)}O_2$ catalysts after DRM reaction (T = 800 °C, CH_4:CO_2:N_2 = 1:1:1, GHSV = 1,620,000 mL·g^{-1}·h^{-1}, and TOS = 10 h).